Flow of Steam-water Mixtures in a Heated Annulus and Through Orifices

JOHN W. HOOPES, JR.
Columbia University, New York, New York

Values of total pressure drop are presented for the flow of vaporizing water in an internally heated 1-in. I.D. by 1¼-in. O.D. annulus at mass velocities of 270 to 1,440 lb./(sec.)(sq. ft.), pressures of 9 to 180 lb./sq. in., and up to 0.34 fraction by weight vaporized. The total heated length over which boiling took place was as large as 6 ft. There is no evidence of "sonic" pressure jumps at the outlet. The results for the annulus mentioned lie within +30 to −11% of the Lockhart-Martinelli curve at higher qualities and with ±45% of the correlation at lower qualities where the actual quality is more uncertain. A simplified correlation in terms of quality and volume fraction of liquid predicted the two-phase frictional pressure drops with an average error of 41%.

It was found that the ratio of the two-phase pressure drop through a 0.3-in. orifice to the drop with no vaporization was approximately a linear function of the quality in the *vena contracta* but was only one tenth to one third as great as would be predicted if the mixture were to expand as a homogeneous fluid. Prediction of orifice pressure drops is improved if slip between vapor and liquid is considered.

Pressure drop accompanying the flow of mixtures of steam and water is of importance in forced- and natural-circulation evaporators, condensate return lines carrying flashing liquids, steam boilers, and certain nuclear reactors. Two-phase flow is also encountered in the simultaneous transport of oil and gas in wells and gathering systems and in air lifts for the pumping of liquids. The resistance offered by restrictions such as valves or orifices, also of interest, has been studied much less than has been flow through uniform conduits. It has commonly been assumed that "critical," or "sonic," conditions occur in vaporizing liquids at surprisingly low flow rates, with large over-all pressure drops resulting because of the accompanying pressure "jump."

This paper discusses two-phase pressure drop data taken in the boiling region of a flow channel in which water was pumped downward through a concentric annulus with an electrically heated core (Figure 1).

APPARATUS

Deionized water was circulated through an air-operated flow-control valve and a measuring orifice and into a 6-in.-diam. header, which served essentially as a high-pressure reservoir at about 250 lb./sq. in. gauge. Flow to the test section, measured by a Potter turbine-type flow meter, was controlled by manually operated valves immediately downstream of the flow meter. The effluent from the test section was quenched by a metered stream of by-pass water, and the combined streams were sent to a booster pump, shell-and-tube heat exchangers, and thence back to the main circulating pump. The pressure in the quench tank was held constant by a standpipe leading to an open drum.

The heated section consisted of an inner tube of 2*S* aluminum approximately 1 in. O.D., pressurized internally with nitrogen, and an outer aluminum housing tube of an outside diameter to give a ⅛- or ¼-in. annulus between them. The annulus concentricity was maintained by spacer ribs made of a silicone-Fiberglas laminate. The ribs were held in broached slots in the housing tube and were in tight contact with the core tube. The resulting annulus, therefore, consisted essentially of three identical subchannels as shown in Figure 2. The heated length over which boiling took place depended on the inlet water temperature but was as long as 6 ft. There was at least an equal length in which liquid was being heated to the boiling point.

The core was heated with direct currents of up to 20,000 amp. In some runs cores having a uniform 0.035-in. wall were used to provide a nearly uniform heat flux over the length of the flow channel. In others cores having a varying wall thickness were used, giving a cosine distribution of heat flux chopped at the ends to about 10% of that at the maximum flux.

At the end of the heated section the annulus was expanded to form the chamber shown in Figure 3. The effluent from the annulus entered the quench tank from the chamber through orifice holes 0.38 in. in diameter. The number of holes could be varied from one to five. Some runs were made with the chamber removed. The annulus effluent then discharged directly into the quench tank.

Pressure taps were located in the quench tank, in the chamber, at the end of the

---

John W. Hoopes, Jr., is at present with Atlas Powder Company, Wilmington, Delaware.
*Tabular material has been deposited as document 5212 with the American Documentation Institute, Photoduplication Service, Library of Congress, Washington 25, D. C., and may be obtained for $2.50 for photoprints or $1.75 for 35-mm. microfilm.

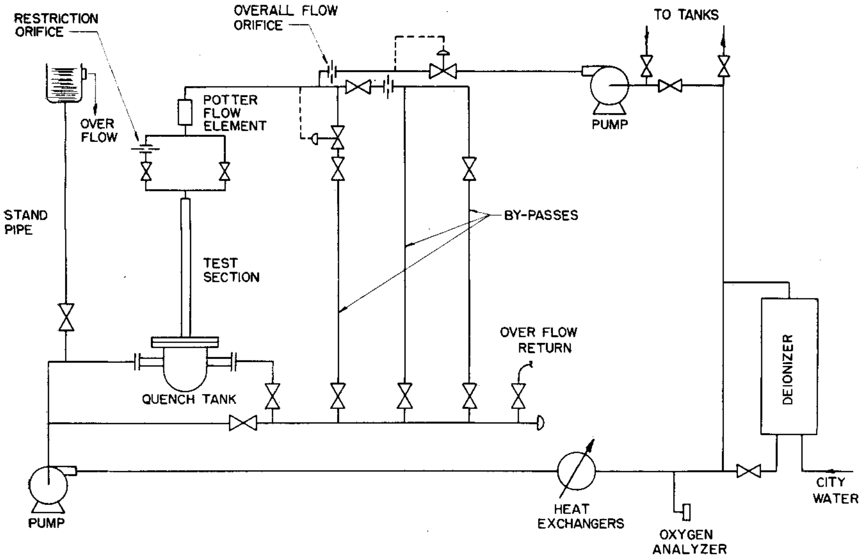

Fig. 1. Sketch of flow loop.

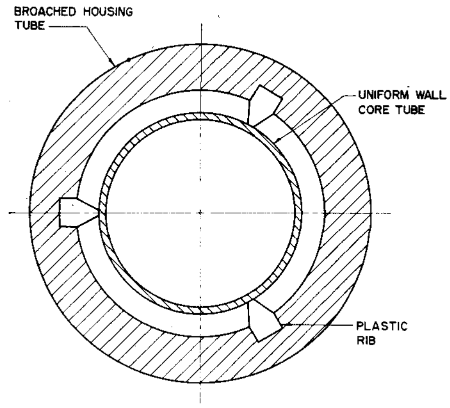

Fig. 2. Cross section of annulus tested.

enlarged section just before the chamber proper, at the annulus outlet, 0.2 ft. upstream, and about every 0.5 ft. for several feet upstream from the outlet. The gauge lines, filled with water at room temperature, led to the manifold shown in Figure 4. All pressures were read on the same 12-in. precision Bourdon gauge shown. [Also visible in the figure are (*a*) the housing tube, (*b*) standpipe, (*c*) nitrogen cylinder, (*d*) bus duct, (*e*) window in quench tank at "4 o'clock" behind the large pressure gauge, (*f*) by-pass.]

Voltage drop and inside wall temperatures were measured over the heated length at cross sections spaced 1.15 ft. apart by use of a rod with thermocouple and voltage probes. This rod was inserted inside the core and manipulated from the top electrical contact assembly. The current, supplied by two generators in parallel, was obtained from the voltage drop across standard shunts. During a given run the current was held constant within ±0.1% by means of an electronic excitation regulator.

The air content of the water during a run was between 2 and 10 p.p.m., usually between 2 and 5 p.p.m.

Accuracy of the important variables is estimated as follows:

Power	±0.25%
Mass velocity	±11 lb.-mass/(sec.)(sq. ft.)
Inlet temperature	±0.5°C.
Pressures	±0.5 lb.-force/sq. in.

Mixture qualities calculated from the preceding data are uncertain by about 0.002. Only results for locations having qualities over about 0.0075 are given here.

The runs reported* were made over the following range of conditions:

Liquid (inlet) velocity, ft./sec.	5.1–19.7
Mass velocity in annulus, lb./(sec.)(sq. ft.)	317–1,230
Outlet quality (uncorrected for kinetic energy)	0.026–0.34
Pressure at start of boiling, lb.-force/sq. in. abs.	41–180
Pressure at annulus outlet, lb.-force/sq. in. abs.	23–83
Pressure in quench tank, lb.-force/sq. in. abs.	23–24
Heat flux at start of boiling (Uniform heat flux runs), B.t.u./(hr.)(sq. ft.)	347,000–864,000

In delineating the two-phase flow region, boiling was assumed to commence at the point where the total energy of the fluid (calculated from the inlet temperature, flow, current, and voltage) was equal to the saturation enthalpy as determined from a plot of pressure and the corresponding enthalpy of saturated liquid along the channel. With the ¼-in. annulus subcooled or local boiling occurred upstream of this point, and a few observations with a glass housing tube with an ⅛-in. annulus have shown that boiling starts near the ribs before the entire liquid is heated to its boiling point. These phenomena cause the pressure gradients to increase above the gradients for all liquid flow before the nominal boiling point is reached but will not be discussed further.

QUALITY

Qualities along the heated section were calculated by setting up a total energy balance between the inlet and the point in question. The total energy E per pound of fluid is given by

$$E = E_i + Q = h_i + \frac{G^2 v_{fi}^2}{2g_c J} + \frac{Z_i g}{g_c J} + Q = h + \frac{Zg}{g_c J} + KE$$

$$= h + \frac{Zg}{g_c J} + \frac{(1-x)G_f^2 v_f^2}{2g_c J} + \frac{xG_g^2 v_g^2}{2g_c J} \qquad (1)$$

Q is the heat added per pound of fluid and was calculated from the flow, current, and voltage drop. Because there may be slip between the two phases of a boiling mixture, with the vapor phase moving faster, the kinetic energies of the liquid and vapor phases are expressed separately in the equation.

If the mixture behaved as a homogeneous fluid—which requires that $V_f = V_g$ and thermodynamic equilibrium exist between the phases—the kinetic energy of the stream could be expressed by a single term similar to that for a pure liquid of specific volume $v = (1 - x)v_f + xv_{fg}$. The kinetic energy term is then merely $(G^2v^2)/2g_c$.

The most convenient way of taking slip velocity into account is to use experimentally measured values of the holdup of liquid and vapor. If this is done, the ratio of the total kinetic energy with slip to that for the homogeneous case is given by

$$\frac{KE}{(KE)_{hom}} = \frac{\dfrac{(1-x)^3 v_f^2}{R_f^2} + \dfrac{x^3 v_g^2}{R_g^2}}{[(1-x)v_f + xv_g]^2} \qquad (2)$$

R_f and R_g are the volume fractions of liquid and vapor respectively and have been correlated by Lockhart and Martinelli (*7*) in terms of the quantity

$$X_{tt} = \sqrt{\frac{(dp/dL)_L}{(dp/dL)_G}} = \chi_{tt}^{0.9}$$

Figure 5*a* was calculated from Equation (2) by use of their correlation; the presence of slip reduces the total kinetic energy by up to 93% at 25 lb./sq. in. abs. The actual kinetic energy may be higher because of the entrainment of some of the liquid in the faster moving gas phase, which has been measured by Alves (*1*).

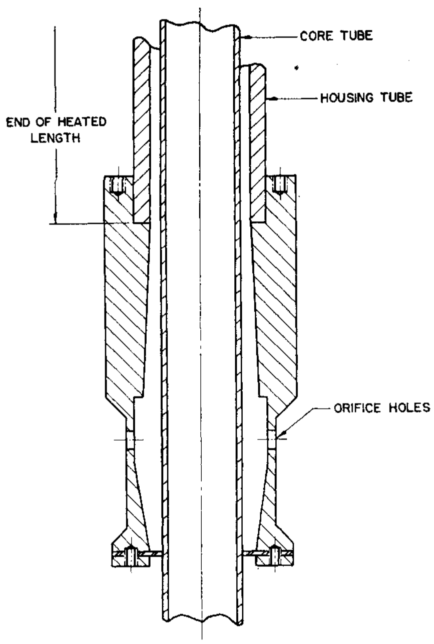

Fig. 3. Annulus outlet and orifice chamber.

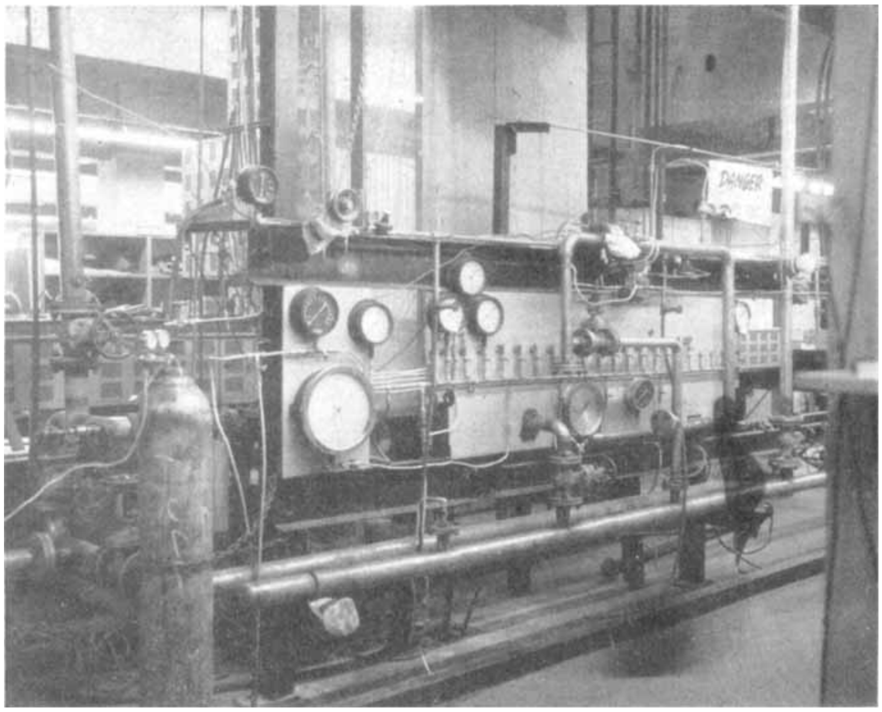

Fig. 4. Photograph of bottom of test section, including pressure manifold.

In general, successive approximations made with Equations (1) and (2) are required to calculate x; however, the kinetic energy terms are small enough to be neglected except at very high mass velocities and low pressures (large v_g). The elevation terms $(Z_i g)/(g_c J)$ and $(Zg)/(g_c J)$ can almost always be neglected.

TYPE OF FLOW

The flow was characterized from the flow-pattern regions given by Baker (*2*) for horizontal flow. As can be seen from Figure 6, at the lowest flow rates the flow pattern theoretically changes in about 2 ft. of channel through the following types of flow: slug, annular, dispersed*. Most of the two-phase pressure drop occurs in the dispersed region. At higher flows with greater turbulence the flow changes from bubble or froth flow directly to dispersed flow.

The conclusions based on Figure 6 are supported by motion pictures of one run, taken through a glass housing tube. Conditions corresponding roughly to the point labeled A on Figure 6 were visually confirmed as bubble or possibly slug flow; however, there were no violent pressure fluctuations commonly attributed to slug flow.

PRESSURE GRADIENTS

The total pressure gradient at any point dp/dL was obtained by taking the slope of a plot of the measured pressures as a function of heated length. By the method of Martinelli and Nelson (*8*), it was then separated by calculation into the following three components:

1. The contribution due to changes in elevation, $(dp/dL)_{EL}$. For downward flow $(dp/dL)_{EL} = -[(R_f/v_f) + (R_g/v_g)]$ which is obtained merely by considering the weight of mixture in a unit height of vertical channel. Since the quantity is small, it was approximated by its value under conditions of homogeneous flow,

$$-\frac{1}{(1-x)v_f + xv_g} = -\frac{1}{v}$$

2. The pressure gradient due to the acceleration or rate of change of momentum of the stream, $(dp/dL)_{ACC}$. A momentum balance for flow patterns typified by annular flow gives

$$\left(\frac{dp}{dL}\right)_{ACC} = \frac{G^2}{g_c}\frac{d}{dL}\left[\frac{(1-x)^2}{R_f}v_f + \frac{x^2}{R_g}v_g\right] = \frac{G^2}{g_c}\frac{dr}{dL} \qquad (4)$$

The values of r, which is a function of quality and pressure, were computed at each point by use of a nomographic chart, plotted, and $(dp/dL)_{ACC}$ was calculated by taking slopes. If the flow were homogeneous,

$$\left(\frac{dp}{dL}\right)_{ACC,hom} = \frac{G^2}{g_c}\frac{d}{dL}[(1-x)v_f + xv_g] \qquad (5)$$

The ratio of the acceleration pressure drop with slip to that for homogeneous flow is plotted in Figure 5*b*, again by use of the Lockhart and Martinelli correlation for R_f and R_g.

3. Frictional pressure gradient $(dp/dL)_{TPF}$ was found by difference. Figure 7 is a typical plot of x, dp/dL, $(dp/dL)_{ACC}$, and $(dp/dL)_{TPF}$ as functions of heated length. Elevation pressure gradients, which ranged from 0.004 to 0.15 lb.-force/(sq. in.)(ft.), are too small to be observable. The fraction of the total pressure drop due to acceleration increases rapidly with increasing quality.

It should be pointed out that at high total pressure gradients the accuracy of the computed frictional drops depends on the accuracy of $(dp/dL)_{ACC}$, which in turn requires accurate values of R_f and R_g. For example, if the acceleration pressure drop had been calculated by Equation (5), the values of $(dp/dL)_{TPF}$ would have been much smaller—or even negative. Thus correlation of two-phase frictional pressure drop under such conditions is a necessary but not sufficient test of the method of calculating $(dp/dL)_{ACC}$ as well as of the correlation method itself. Unfortunately, if correlations fail it is difficult to isolate the cause.

*Baker in his review summarizes various investigators' definitions of these types of flow as follows: *slug flow*, flow in which a wave is picked up periodically by the more rapidly moving gas to form a frothy slug which passes through the pipe at a much greater velocity than the average liquid velocity; *annular flow*, flow in which the liquid forms in a film around the inside wall of the pipe and the gas flows at a high velocity as a central core; *dispersed flow*, flow in which most or nearly all of the liquid is entrained as spray by the gas.

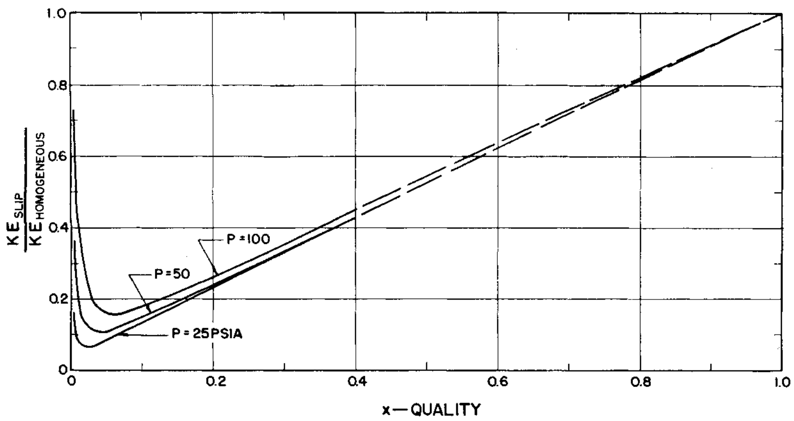

Fig. 5*a*. Ratio of kinetic energy, slip velocity being taken into account, to the kinetic energy for homogeneous flow.

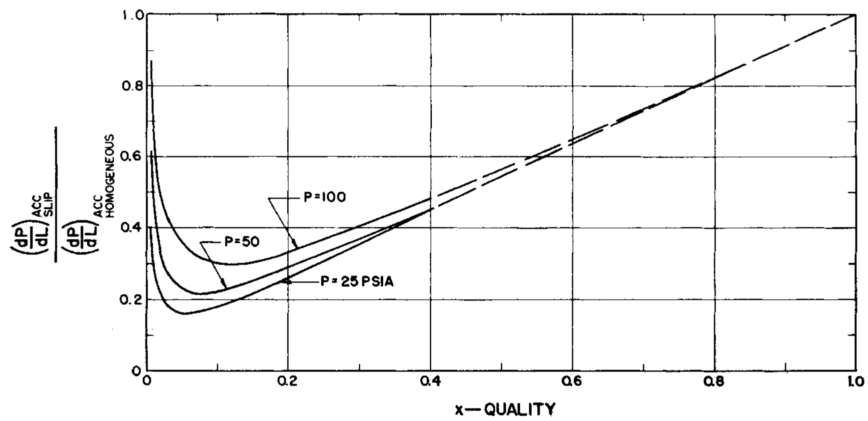

Fig. 5*b*. Ratio of acceleration pressure gradient, slip velocity being taken into account, to the acceleration pressure gradient, homogeneous flow being assumed.

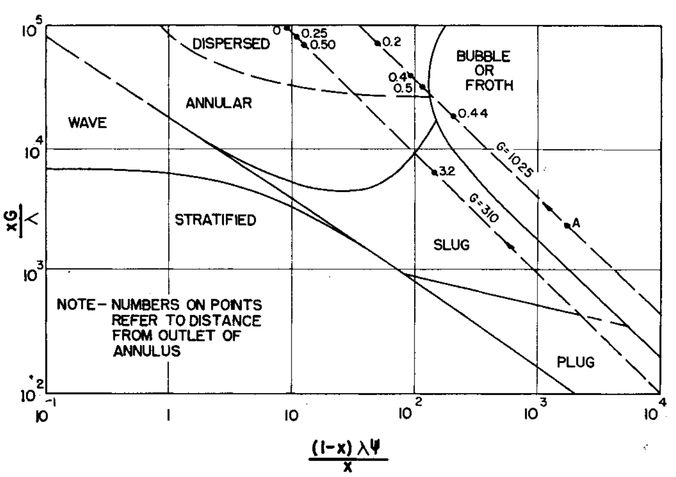

Fig. 6. Flow-pattern regions for results reported (correlation of Baker).

LOCKHART AND MARTINELLI CORRELATION FOR TWO-PHASE FRICTIONAL PRESSURE DROP

Values of $(dp/dL)_{TPF}$ were calculated from several points along the tube for twenty-two different runs. They were converted to the Lockhart and Martinelli parameter $\phi_L = [(dp/dL)_{TPF}/(dp/dL)_L]^{1/2}$ by no-power liquid–pressure-drop data for calculating $(dp/dL)_L$ and were plotted as a function of χ_{tt}. Figure 8 shows that the results for the ⅛-in. annulus lie within +30 to −11% of the Lockhart-Martinelli curve at higher qualities (lower χ_{tt}) and within ±45% of the correlation at lower qualities (higher χ_{tt}), where the actual quality is in doubt by as much as 20 to 30%. It should be remembered that errors of +30 or ±45% in ϕ_L correspond to +70 or +110 to −70% error in the calculated pressure drop respectively. No satisfactory explanation for the higher deviation of the two ¼-in. runs has been advanced.

SIMPLIFIED CORRELATION FOR VAPORIZATION PROCESSES

Calculation of two-phase frictional-pressure drop when a liquid is being heated and vaporized in the same conduit is more convenient if the frictional-pressure gradient is expressed as the ratio $(dp/dL)_{TPF}/(dp/dL)_f$; where $(dp/dL)_f$ is the pressure gradient that would be obtained if all the mixture were liquid at the same temperature, and it is very nearly constant along the tube. The Lockhart and Martinelli $(dp/dL)_L$ is approximately equal to $(dp/dL)_f$ $(1 - x)^{1.8}$.

The results of Linning (*6*) indicate that in annular flow, which is closely related to dispersed flow, the vapor-liquid–interface velocity is approximately equal to that of the average liquid velocity. Thus in downward flow in a pipe the liquid near the wall behaves essentially as a falling film whose flow is aided by the more rapidly moving gas but whose "wetted perimeter" for friction is the conduit wall perimeter, the same as it would be if the channel were full of liquid. It seems reasonable therefore to consider the pressure drop due to the "actual" liquid velocity. In a narrow annular passage or closely spaced parallel plates the wetted area may decrease as the quality increases, as vapor may tend to flow near to one wall of the passage.

If a friction factor f_{TPf} for the liquid phase alone is defined by the usual Fanning equation, the equation for frictional pressure gradient can be written for the liquid phase and for the total flow if it were all liquid. Division of the two equations gives

$$\frac{(dp/dL)_{TPF}}{(dp/dL)_f} = \left(\frac{f_{TPf} r_{HTPf}}{f_f r_H}\right)\left(\frac{1 - x}{R_f}\right)^2 \quad (6)$$

where r_{HTPf} and r_H are the hydraulic radii (ratio of cross-sectional area to wetted perimeter) of the liquid phase in the mixture and of the completely filled flow channel. Calvert and Williams (*9*) have treated this problem more elegantly by considering the shear forces in the liquid phase.

Presumably the product $f_{TPf} r_{HTPf}$ is a function of the flow pattern, slip velocity, and quality. On the other hand the plot of the pressure-gradient ratio in Figure 9 as a function of $[(1 - x)/R_f]^2$ shows that the results with the ⅛-in. annulus can be correlated with an average deviation of 41% by assuming $(f_{TPf} r_{HTPf})/(f_f r_H) = 1$ in Equation (6).

Since the ratio r_{HTPf}/r_H would be equal to R_f if the wetted perimeter were to remain unchanged during the vaporization, this assumption could hold true only if the walls were becoming partially nonwetted as quality increased.

Figure 9 is also interesting in that the published values of R_f and R_g are used to estimate phase velocities in the annular- and dispersed-flow region and indicate that a large part of the increased pressure drops in two-phase flow can be accounted for by the increased velocities of the phases. The effect of wave formation as found by Bergelin *et al.* (*5*) for stratified flow is probably not a factor here in the annular and dispersed region, although entrainment is the analogous effect in annular flow.

Those points on the right of Figure 9, in which the observed frictional pressure drop is greater than 200% of that predicted correspond to runs with medium flow (G = 400 to 1,000 lb.-mass/(sec.)(sq. ft.) and of fairly high quality (greater than 0.1) and to locations only about 0.25 ft. from the annulus outlet. At this location the pressure gradient is quite steep, about 100 lb.-force/(sq. in.) ft. $(dp/dL)_{TPF}$ is probably high for two reasons: (1) the calculated $(dp/dL)_{ACC}$ is probably too low because entrainment of some of the liquid in faster moving vapor is not taken into account [if $(dp/dL)_{ACC}$ were higher, then $(dp/dL)_{TPF}$ would be smaller] and (2) the extra energy required to detach and accelerate liquid droplets from the bulk of the liquid undoubtedly shows as added pressure drop.

The two very low points on the right half of Figure 9 are for two runs of high flow [G > 1,100 lb.-mass/(sec.)(sq. ft.)] and low quality (less than 0.05). Along a large part of the heated length $(dp/dL)_{ACC}$, as calculated by Equation (4), is greater than dp/dL. The calculated acceleration pressure drops may be high because of a failure to maintain thermodynamic equilibrium at these high flows. If this were true, the calculated rate of change of quality would be too high, which would be reflected in a too-high $(dp/dL)_{ACC}$.

Since the Lockhart-Martinelli parameter χ_{tt} must be evaluated in order to find R_f, the utility of the correlation rests primarily in the convenience of using the ratio $(dp/dL)_{TPF}/(dp/dL)_f$ where the quality is changing.

SONIC OR CRITICAL VELOCITY

The pressure at the annulus outlet was found to be very near that of the orifice chamber (or of the quench tank if the chamber were removed) in every boiling run. There was no evidence of sonic choking at the outlet, even at the highest flows and very steep pressure gradients. The flows were up to four times as high as the critical mass velocity calculated

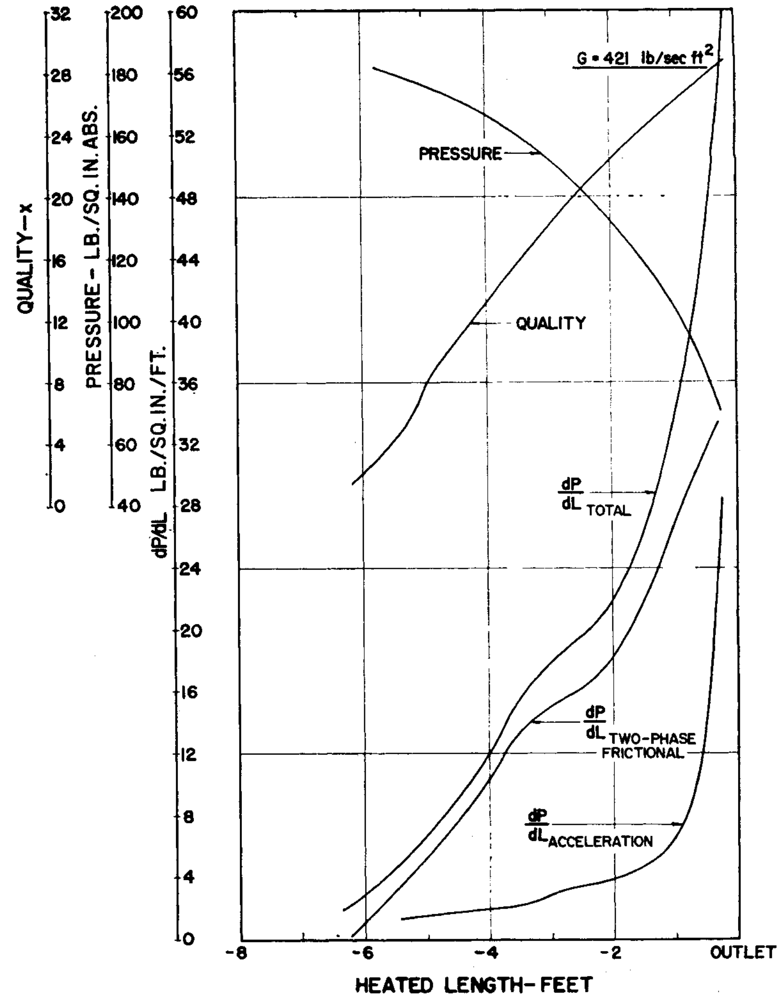

Fig. 7. Plot of quality, total pressure gradient, and acceleration pressure gradient as a function of heated length.

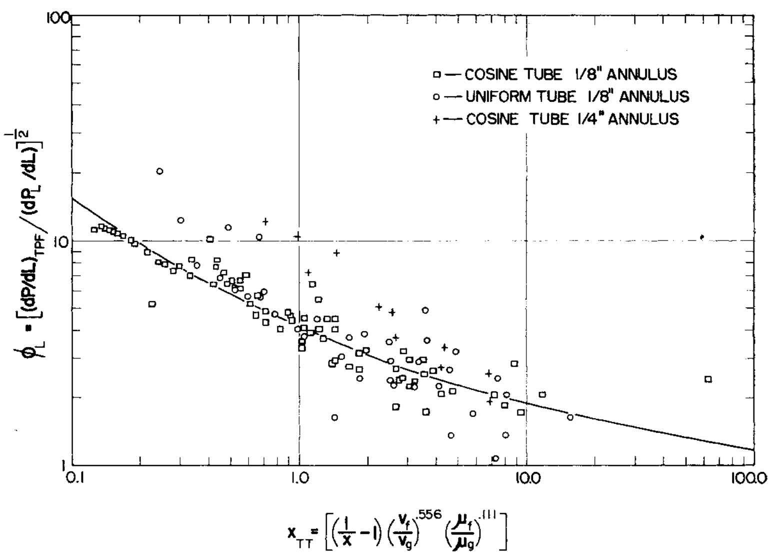

Fig. 8. Plot of Martinelli parameter ϕ_L as a function of χ_{tt}.

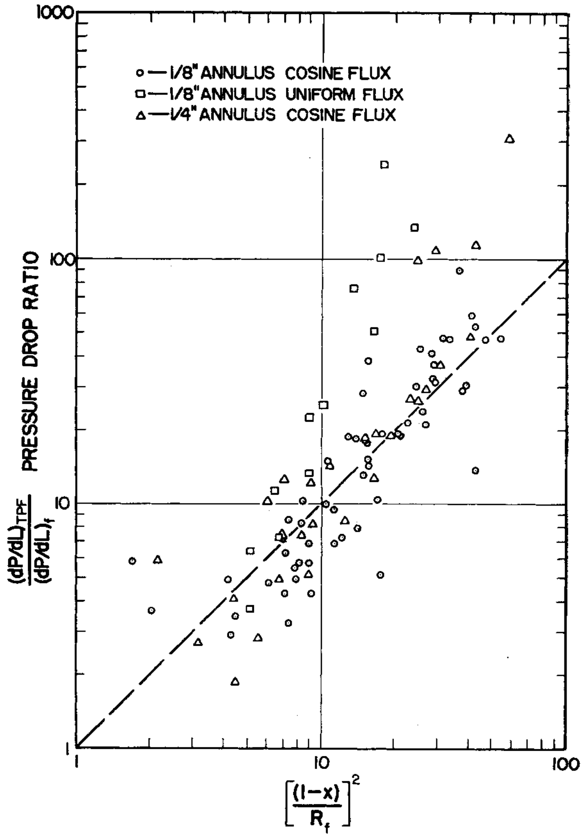

Fig. 9. Plot of two-phase frictional pressure-drop ratio $(dp/dL)_{TPF}/(dp/dL)_f$ as a function of $(1-x)^2/R_f^2$.

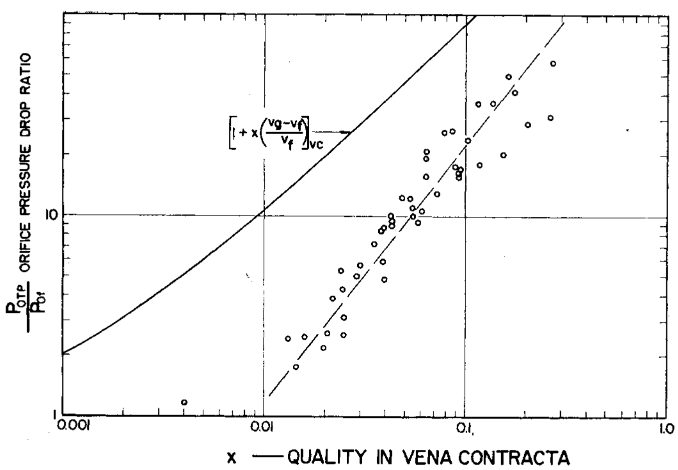

Fig. 10. Plot of two-phase orifice pressure-drop ratio $\Delta p_{OTP}/\Delta p_{Of}$ as a function of x_{VC}, homogeneous flow being assumed.

when a homogeneous fluid was assumed at outlet conditions:

$$G_{crit} = \sqrt{-g_c\left(\frac{\partial p}{\partial[(1-x)v_f + xv_g]}\right)_s} \qquad (7)$$

The very steep pressure gradients at the outlet may have been interpreted by previous investigators as a choking due to critical flow. Indeed, the practical effect may be considered to be the same as if a "jump" had occurred, as the over-all pressure drop for a given flow and power input was essentially unaffected by removal of the chamber, i.e., by a change in annulus discharge pressure. In calculating over-all pressure drops by steps or by graphical integration using the equation

$$p_1 - p_2 = \int_{L_1}^{L_2} (dp/dL)_{TPF}\, dL + \int_{L_1}^{L_2} (dp/dL)_{ACC}\, dL + \int_{L_1}^{L_2} (dp/dL)_{EL}\, dL \qquad (8)$$

one can assume the outlet pressure to be that at which Equation (7) applies. A graphical representation of Equation (7) is available for steam-water mixtures (*10*).

PRESSURE DROP THROUGH ORIFICES

The pressure drop across an orifice discharging into a large chamber is the acceleration pressure drop between the upstream side and the *vena contracta.* For homogeneous flow this would be equal to $G^2v/2g_c$, evaluated at the *vena contracta* conditions. There is no regain of pressure because the energy of the jet is completely lost in turbulence.

If the upstream velocity in the direction of the orifice is negligible, the ratio of the pressure drop for a *homogeneous* two-phase mixture to that for liquid at the same mass velocity and temperature is given by

$$\frac{\Delta p_{OTP,hom}}{\Delta p_{Of}} = \frac{(1-x)v_f + xv_g}{v_f} = 1 + \frac{x(v_g - v_f)}{v_f} \qquad (9)$$

If slip is taken into account, the pressure drop is equal to $r(G^2/g_c)$ where r is defined in Equation (4). Expressed as a pressure-drop ratio,

$$\frac{\Delta p_{OTP}}{\Delta p_{Of}} = \frac{(1-x)^2}{R_f} + \frac{v_g}{v_f}\frac{x^2}{R_g} \qquad (10)$$

Values of Δp_{Of} were obtained from the results of runs with cold water, suitably corrected to the saturation temperature at the quench tank (*vena contracta*) pressure. The cross-sectional area of the *vena contracta* was taken as 61% of the orifice area, as determined by these measurements. With this value of the area, kinetic energy corrections were applied to the total energy when qualities were calculated.

Figure 10 is a plot of the orifice-pressure-drop ratio as a function of quality evaluated at quench-tank conditions. Since the quench-tank pressure was essentially the same for all runs, v_g and v_f are the same, and Equation (9) can be shown as a single curve. The assumption of homogeneous flow leads to predicted pressure drops from 400 to 900% of those observed. Quality alone serves to correlate the results well; however, the points from a series of runs at a quite different quench-tank pressure would probably have fallen on a different line.

Figure 11*a* shows that Equation (10) agrees much better with the experimental results than does Equation (9). Qualities are calculated by use of Equations (1) and (2) to evaluate the kinetic energy in Figure 11*a*. The predicted pressure drops are progressively lower at higher powers, i.e., at higher flow rates for a given quality. In Figure 11*b* the homogeneous *kinetic* energy was used in the energy balance at higher flows to calculate the qualities. It is seen that the effect of power is eliminated. The average error is 31%. The very low points are for low qualities (about 0.02) where quality may be in error by 10% and flow patterns may not be the same as for higher degrees of vaporization. In any case the agreement is surprisingly good considering that the values of R_g and R_f used were those for horizontal flow of air and water or air and kerosene through a uniform pipe.

There was apparently no "sonic choking" due to critical flow. This agrees with the results of Benjamin and Miller (*4*), who passed steam-water mixtures through orifices at pressure differences up to 145 lb./sq. in. gauge.

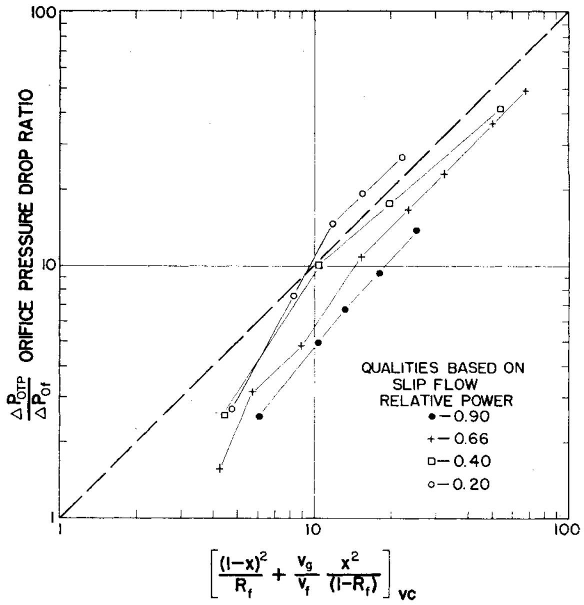

Fig. 11*a*. Plot of two-phase orifice pressure-drop ratio $\Delta p_{OTP}/\Delta p_{Of}$ as a function of $[(1-x)^2/R_f] + (v_g/v_f)(x^2/R_g)$, qualities based on slip flow at *vena contracta* conditions.

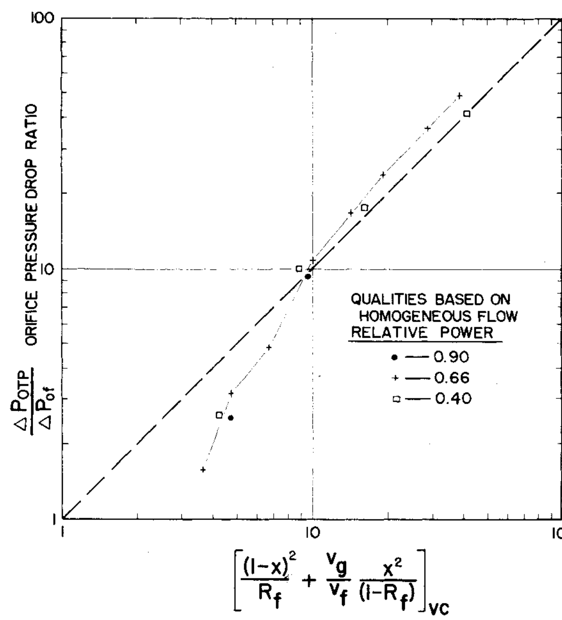

Fig. 11*b*. Plot of two-phase orifice pressure-drop ratio $\Delta p_{OTP}/\Delta p_{Of}$ as a function of $[(1-x)^2/R_f] + (v_g/v_f)(x^2/R_g)$, qualities based on homogeneous flow at *vena contracta* conditions.

CONCLUSIONS

The results indicate that the relationships given by Martinelli and Nelson (*8*) for calculating local two-phase pressure gradients of vaporizing water are satisfactory for a small annulus and downward flow in the dispersed and slug-annular flow regions and the relatively low pressures used in this study. More data are desirable on larger diameter flow channels in vertical conduits.

The correlation of Lockhart and Martinelli for volume fraction vapor and liquid in horizontal flow can be used to estimate pressure drops for flow of flashing mixtures through orifices with an average error of 31%. At qualities over about 0.05, the error is about 20%. The correlation is also useful in calculating frictional pressure drop in pipes, an indication that the individual phase velocities are the chief factor determining the frictional pressure drop in the flow regions studied.

A better understanding of the phenomena involved, which will presumably result in an ability to predict pressure drops more accurately, can best be obtained by measurements of flow pattern with visual observations and of local slip velocities or holdup.

ACKNOWLEDGMENT

The author wishes to acknowledge the help of Martin Gutstein and William Begell in performing many of the calculations and of Henry Hyman in preparing the drawings.

NOTATION

E = total specific energy of stream, B.t.u./lb. mass
f = Fanning friction factor $\dfrac{(dp/dL)_F}{\dfrac{r_H V^2}{2g_c}}$
G = mass velocity, lb.-mass/(sec.)(sq. ft.)
g_c = gravitational conversion factor, (lb.-mass/ft.)(lb. force/sec.²)
g = local acceleration of gravity, ft./sec.²
h = specific enthalpy, B.t.u./lb.-mass
J = conversion factor, (ft.)(lb.)/B.t.u.
L = heated length, measured in direction of flow, ft.
p = static pressure, lb.-force/sq. in. abs.
Q = heat added to stream along L feet, B.t.u./lb. mass
r_H = hydraulic radius, cross sectional area divided by wetted perimeter, ft.
R = fraction of cross section occupied by a phase
s = entropy, B.t.u./(lb.-mass)(°F.)
S = cross section perpendicular to flow, sq. ft.
v = specific volume, cu. ft./lb.-mass
V = velocity, ft./sec.
W = mass rate of flow, lb.-mass/sec.
x = quality (W_g/W)
X_{tt} = Lockhart and Martinelli correlating parameter = $\sqrt{\dfrac{(dp/dL)_L}{(dp/dL)_G}}$ for both phases turbulent
Z = elevation above arbitrary datum, ft.

χ_{tt} = Lockhart and Martinelli correlating parameter = $X_{tt}^{1/1.9}$
ϕ_L = Lockhart and Martinelli parameter =

$$\sqrt{\frac{(dp/dL)_{TPF}}{(dp/dL)_L}}$$

λ = $[(0.075v_g)(62.3v_f)]^{-1/2}$
Ψ = $(73/\nu)[\mu_f(62.3v_f)^2]^{1/3}$
ν = surface tension of liquid phase, dynes/cm.

Subscripts

f = saturated liquid phase
g = saturated vapor phase
i = initial (subcooled) conditions
Absence of a subscript usually denotes an average property for the whole stream, such as $W = W_f + W_g$, $v = (1 - x)v_f + xv_{fg}$
O = orifice (used with other subscripts)
TP = two phase
hom = homogeneous flow
crit = critical or sonic conditions
vc = *vena contracta*

Pressure Gradients, lb.-force/(sq. ft./ft.)

dp/dL = static pressure gradient
$(dp/dL)_{ACC}$ = acceleration pressure gradient
$(dp/dL)_{EL}$ = gradient due to elevation differences
$(dp/dL)_{TPF}$ = two-phase frictional pressure gradient for whole stream (W lb.-mass/sec.)
$(dp/dL)_L$ = pressure gradient if only the liquid phase were flowing (W_f lb.-mass/sec., as a liquid)
$(dp/dL)_G$ = pressure gradient if only the vapor phase were flowing (W_g lb.-mass/sec., as a vapor)
$(dp/dL)_f$ = pressure gradient if the whole stream were flowing as a liquid (W lb.-mass/sec.)
Δp_{OTP} = two-phase orifice pressure drop (W lb.-mass/sec.)
Δp_{Of} = orifice pressure drop if W lb. mass/sec. of liquid were flowing

LITERATURE CITED

1. Alves, G. E., *Chem. Eng. Progr.*, **50**, 449 (1954).
2. Baker, Ovid, *Oil Gas J.*, p. 185 (July 26, 1954).
3. Begell, William, and J. W. Hoopes, Jr., "Acceleration Pressure Drops in Two-phase Flow," internal report (April 1954).
4. Benjamin, M. W., and J. G. Miller, *Trans. Am. Soc. Mech. Engrs.*, **63**, 419 (1941).
5. Bergelin, O. P., P. K. Kegel, F. G. Carpenter, and Carl Gazley, Jr., "Heat Transfer and Fluid Mech. Institute," p. 19, Am. Soc. Mech. Engrs. (1949).
6. Linning, D. L., *Proc. Inst. Mech. Engrs., (London)*, 1B, 64 (1952).
7. Lockhart, R. W., and R. C. Martinelli, *Chem. Eng. Progr.*, **45**, 39 (1949).
8. Martinelli, R. C., and D. B. Nelson, *Trans. Am. Soc. Mech. Engrs.*, **70**, 695 (1948).
9. Calvert, Seymour, and B. C. Williams, *A.I.Ch.E. Journal*, 1, 78 (1955).
10. "The Reactor Handbook," vol. 2, p. 77, AECD-3546, Govt. Printing Office, Washington, D. C. (March 1955).

APPENDIX

Derivation of Equations

Kinetic Energy

The kinetic energy per pound of a homogeneous fluid or of a single phase of a mixture can be expressed by

$$KE = \frac{V^2}{2g_cJ} = \frac{G^2v^2}{2g_cJ} = \frac{W^2v^2}{S^2 2g_cJ} \quad (10)$$

if the velocity profile is sufficiently flat. The average specific volume v of a two-phase mixture at rest or with phases moving at the same velocity is given by

$$v = (1 - x)v_f + xv_g \quad (11)$$

Thus the expression for kinetic energy becomes for homogeneous flow

$$KE = \frac{G^2[(1 - x)v_f + xv_g]^2}{2g_cJ} \quad (12)$$

In general, if $V_f \neq V_g$,

$$V_f = \frac{W_f v_f}{R_f S} = \frac{(1 - x)Wv_f}{SR_f}$$

$$= (1 - x)\frac{v_f}{R_f}G \quad (13a)$$

$$V_g = \frac{W_g v_g}{R_g S} = \frac{xWv_g}{SR_g} = x\frac{v_g}{R_g}G \quad (13b)$$

and the total kinetic energy per pound of mixture for flow with slip is then [from Equation (1)]

$$KE = \frac{G^2}{2g_cJ}\left[(1 - x)^3\frac{v_f^2}{R_f^2} + \frac{x^3v_g^2}{R_g^2}\right] \quad (14)$$

Division of Equation (14) by (12) gives Equation (2).

Elevation Head

The head drop due to a change in elevation is calculated from the weight of the mixture which is included within cross sections ΔZ apart.

The mass of liquid included in a length ΔL is equal to $R_f S\Delta L/v_f$, and the mass of vapor is $R_g S\Delta L/v_g$. The component of the force of gravity acting in the direction of flow is then equal to

$$\left[\frac{R_f}{v_f} + \frac{R_g}{v_g}\right]S\Delta L\,\frac{g}{g_c}\left(\frac{\Delta Z}{\Delta L}\right)$$

Expressed as a pressure gradient by dividing by $S\Delta L$ and letting ΔL become very small

$$\left(\frac{dp}{dL}\right)_{EL} = \left[\frac{R_f}{v_f} + \frac{R_g}{v_g}\right]\frac{g}{g_c}\left(\frac{\Delta Z}{\Delta L}\right) \quad (15)$$

g/g_c is equal to unity. For vertically downward flow

$$\frac{\Delta Z}{\Delta L} = -1$$

and Equation (3) results.

For a homogeneous fluid the mass of fluid included between the sections is merely $S\Delta L/v$, where v is given by Equation (11). Reasoning analogous to that used in deriving Equation (3) gives the expression

$$\left(\frac{dp}{dL}\right)_{EL,hom} = -\frac{1}{(1 - x)v_g + xv_g} \quad (16)$$

Acceleration Pressure Drop

The pressure gradient due to acceleration is the rate of change with distance of the rate of momentum carried by the fluid, divided by the cross section. For a homogeneous fluid, momentum is carried past a cross section at a *rate* given by

$$\frac{WV}{g_c} = \frac{WGv}{g_c} \quad (17)$$

measured in pounds force. The acceleration pressure drop is obtained by taking the rate of change of this momentum flow with distance and dividing by the cross section. Equation (5) is obtained if v is evaluated by Equation (11).

The total rate of flow of momentum carried by a two-phase mixture is similarly found to be

$$\frac{W_fV_f}{g_c} + \frac{W_gV_g}{g_c} \quad (18)$$

Substitution of

$$W_f = (1 - x)W \quad (19)$$

$$W_g = xW \quad (20)$$

$$V_f = \frac{(1 - x)Wv_f}{R_f S}$$

$$= (1 - x)\,G\frac{v_f}{R_f} \quad (21)$$

$$V_g = \frac{xGv_g}{R_g} \quad (22)$$

differentiating and dividing by S gives Equation (4).

Application of Fanning Equation to Individual Phases

The Fanning equation for all liquid flow can be written as

$$\left(\frac{dp}{dL}\right)_f = \frac{f_f r_H V^2}{2g_c v_f} = \frac{f_f r_H W^2 v_f}{2g_c S^2} \quad (23)$$

A similar equation can be written for the liquid phase alone in two-phase flow

$$\left(\frac{dp}{dL}\right)_{TPf} = \frac{f_{TPf} r_{HTPf} V^2{}_{TPf}}{2g_c v_f}$$

$$= \frac{f_{TPf} r_{HTPf}(1 - x)^2 W^2 v_f}{2g_c(R_f S)^2} \quad (24)$$

Thus the two-phase-pressure-drop ratio is obtained by division of Equation (24) by Equation (23).